FINITE-DIFFERENCE TIME DOMAIN METHOD SOURCE CALIBRATION FOR HYBRID ACOUSTICS MODELING

Samuel Siltanen, Alex Southern, and Lauri Savioja

Aalto University School of Science
Department of Media Technology
P.O. Box 15500 FI0076 Aalto

ABSTRACT

Finite-difference time domain methods are commonly used for acoustics modeling of enclosed geometries. For large spaces and high frequencies, the computational requirements become prohibitive in practical use. Thus, geometric acoustics algorithms are used in those cases. The results of these two classes of algorithm can be combined to model the full acoustic response. To allow direct mixing of the results, the source strengths should be calibrated. This paper derives calibration factors for various finite-difference time domain methods. It is shown that the modelled acoustics responses can then be easily combined to synthesise wide-band hybrid responses.

Index Terms— Acoustic emission, Acoustic propagation, Acoustic signal processing, Room acoustics, Finite-difference time domain methods

1. INTRODUCTION

When the goal is to model room acoustics, there are several methods available. In some algorithms, the wave equation is solved numerically. This can be achieved by discretizing the room boundaries, yielding a boundary element method (BEM), or discretizing the room volume, yielding a finite element method (FEM). In these cases the discretization is usually only spatial and the solution is obtained in the frequency domain, although exceptions exist. A spatio-temporal approximation of the wave equation may be obtained by representing the continuous propagation medium with a discrete set of points, called *nodes*. This approach leads to finite difference time domain (FDTD) methods where the processing is performed in the time domain and the calculations are relatively simple compared to BEMs or FEMs.

Often the computing time, available computing power and memory are limiting the use of the aforementioned methods to low frequencies. Thus, geometric acoustics modeling algorithms are most practical at higher frequencies. They assume that sound travels along straight paths or rays. While this is not physically accurate, the approximation is often sufficiently close to the reality at higher frequencies.

If the contradicting requirements of physical accuracy and efficient computing are combined, it is reasonable to use a hybrid approach where the wave-based methods (BEM / FEM / FDTD) are used at low frequencies and the geometric methods at high frequencies. In the end, the modeling results are combined to obtain the full-band impulse responses in the given room.

Since the geometric modeling is most often computed in the time domain, it is simplest to also use time-domain modeling at the low frequencies. Then FDTD methods are the most obvious choice. Of course, it is possible to use frequency-domain methods and then use the Fourier transform to switch the responses to the same domain. But this paper concentrates on how to combine the FDTD modeling results with the geometric modeling results. The calibration coefficients are also required when the responses of different FDTD schemes are to be compared directly.

1.1. Previous Work

Kowalczyk and van Walstijn have listed seven different FDTD schemes that could be presented in one unified framework [1]. Their classification of the FDTD methods is used in this paper. On the other hand, Siltanen et al. generalize the geometric methods under one equation [2]. Thus, the choice of the exact geometric algorithm is not critical as they should ultimately produce the same results.

There have been several implementations combining two geometric modelling approaches [5],[6],[7]. Also, the idea of splitting the modelling task between the wave-based methods and the geometric methods has already been suggested in, e.g. [8], and more recently in [9]. Only recently, has there been complete implementations combining two approaches [10],[11],[12].

The calibration parameter defined in this paper is applicable to previously presented hybrid acoustic models. Murphy et al. presented a hybrid acoustic model based on a combination of ray-tracing and the Digital Waveguide Mesh (DWM), which is closely related to FDTD method [10]. A 3-D and 2-D DWM was employed for synthesizing the early and late parts of the impulse response respectively. A more recent hybrid model presented by Southern et al. uses a combination of FDTD, Beam-Tracing and the Acoustic Radiance Transfer methods for impulse response synthesis [12]. In addition that work presented three methods for performing the calibration discussed in this work. Only one of the methods had the acoustically physical foundation that is desired for accurate hybrid impulse response synthesis. The main disadvantage of that approach was that the calibration operation required a direct line of sight between source/receiver and the accuracy was dependent on the ability to window the direct sound. These restrictions are alleviated using the method presented in this paper.

2. SOURCE CALIBRATION

For geometic modeling techniques, it is trivial to set the omnidirectional sound source strength so that it produces intensity $I = 1W/m^2$ at some distance R. Given a sound source with strength P,

$$I = \frac{P}{4\pi R^2}. \tag{1}$$

Or if the calculations are done with pressures:

$$p = \sqrt{\frac{PZ}{4\pi R^2}} = \sqrt{\frac{PZ}{4\pi}}/R, \tag{2}$$

where Z is the acoustic impedance of the medium. Obviously, there is $1/R$-dependence in pressures. Here, both power and pressure are defined in the root mean square sense.

On the other hand, in FDTD simulations, sound is excited from the source and propagated in a grid. Pressure values are stored at each node and those values are updated in discrete time steps. The general update equation is shown in Eq 3 [1], where $p^n_{l,m,i}$ is the update variable at node position $\{l, m, i\}$ in the 3-dimensional grid, and n is the time index. Constants d_1, d_2, d_3, and d_4 depend on the scheme and are listed in Table 1.

Without loss of generality, a delta-like source signal is considered. The grid cell corresponding to the sound source is set to unity at time index $n = 0$ and then the sound is propagated in the grid by using the update equations of that particular FDTD scheme.

This FDTD sound source initialization has no obvious physical interpretation. In the following, the sound source strength in FDTD techniques is adjusted so that it matches the geometric sound source strength.

All FDTD methods use a grid with some inter-nodal spacing X. The grid spacing is related to the sampling rate f_s and the Courant number λ that depends on the chosen scheme [1]:

$$X = \frac{c}{f_s \lambda}. \tag{4}$$

It is possible to calculate the geometric sound source pressure level at distance X from the source. Obviously,

$$p = \sqrt{\frac{PZ}{4\pi}}/X. \tag{5}$$

On the other hand, many FDTD techniques calculate the sound pressure at that distance for the nodes next to the source. However, only part of the frequency range is valid, and in some FDTD schemes the nodes next to the source remain zero. Thus, the FDTD node values cannot be directly compared to the geometric pressure values at the corresponding positions.

The FDTD signal must be low-pass filtered to make the comparison meaningful. In this comparison, the whole valid frequency range of the FDTD schemes is not required. Ultimately, it is sufficient to compare the DC level of the FDTD results to the geometric pressure levels. This is the same as the total accumulated value of the FDTD signal at the receiver point, i.e.

$$p_{DC} = \sum_{n=1}^{\infty} p^n_{l,m,i}, \tag{6}$$

where $p^n_{l,m,i}$ is the observed pressure value at receiver node l, m, i at time sample n when using the notation in [1]. Even when the initial source excitation is the same, p_{DC} will have different values depending on the scheme.

It is difficult to derive an analytical expression for the received signal, and so far it has been done only in the 2-dimensional case [3]. Thus, simulations are performed to determine the ratio between the source excitation level and the DC level of the signal at the receiver position, i.e.

$$A = \frac{p_{DC}}{p_{init}}. \tag{7}$$

Most often $p_{init} = 1$. Table 1 lists these ratios, hereafter called calibration coefficients. In the simulations, each FDTD scheme is run for a source in free space with a sufficiently large grid to avoid any reflections. The pressure values at the receiver position are accumulated as in Eq. 6. The receiver positions are one node away from the source in all but the octahaedral and cubic close-packed schemes, where those nodes remain zero throughout the simulation. In those cases, the receivers were two nodes away from the source. In the end, the coefficients are scaled back as if the source was just one node away from the source.

The total calibration factor is

$$\eta = \frac{R\lambda f_s}{Ac} = \frac{R}{AX}, \tag{8}$$

where R is the distance at which the geometric sound source has intensity 1 W/m^2, λ is the Courant number (see Table~1), f_s is the sampling rate, c is the speed of sound, and A is the calibration coefficient.

3. EXAMPLES

It is well-known that geometric methods do not capture the wave phenomena such as diffraction. Thus, to avoid extra considerations related to the validity of the geometric results,

$$
\begin{aligned}
p^{n+1}_{l,m,i} \; = \; & d_1(p^n_{l+1,m,i} + p^n_{l-1,m,i} + p^n_{l,m+1,i} + p^n_{l,m-1,i} + p^n_{l,m,i+1} + p^n_{l,m,i-1}) \\
& + d_2(p^n_{l+1,m+1,i} + p^n_{l+1,m-1,i} + p^n_{l+1,m,i+1} + p^n_{l+1,m,i-1} + p^n_{l,m+1,i+1} + p^n_{l,m+1,i-1} \\
& \; + p^n_{l,m-1,i+1} + p^n_{l,m-1,i-1} + p^n_{l-1,m+1,i} + p^n_{l-1,m-1,i} + p^n_{l-1,m,i+1} + p^n_{l-1,m,i-1}) \\
& + d_3(p^n_{l+1,m+1,i+1} + p^n_{l+1,m+1,i-1} + p^n_{l+1,m-1,i+1} + p^n_{l+1,m-1,i-1} \\
& \; + p^n_{l-1,m+1,i+1} + p^n_{l-1,m+1,i-1} + p^n_{l-1,m-1,i+1} + p^n_{l-1,m-1,i-1}) + d_4 p^n_{l,m,i} - p^{n-1}_{l,m,i}. \qquad (3)
\end{aligned}
$$

Table 1. Calibration coefficients for different 3-D FDTD schemes extended from [1].

	Std. Rect.	Octa-hedral	Cubic Close-Packed	Interp. DWM	Interp. Isotropic	Isotropic 2	Interp. Wideb.
λ	$\sqrt{\frac{1}{3}}$	1	1	$\sqrt{\frac{1}{3}}$	$\sqrt{\frac{3}{4}}$	$\sqrt{\frac{3}{4}}$	1
d_1	$\frac{1}{3}$	0	0	0.1205	$\frac{1}{4}$	$\frac{15}{48}$	$\frac{1}{4}$
d_2	0	0	$\frac{1}{4}$	0.0386	$\frac{1}{8}$	$\frac{3}{32}$	$\frac{1}{8}$
d_3	0	$\frac{1}{4}$	0	0.0146	0	$\frac{1}{64}$	$\frac{1}{16}$
d_4	0	0	-1	0.6968	-1	$-\frac{9}{8}$	$-\frac{3}{2}$
A	0.3405	0.2090	0.1708	0.2399	0.2372	0.2544	0.2089

a simple "shoebox" model is chosen for this initial examination. In this case, there are no diffracting edges and the solution is exact, assuming the walls are rigid, and the responses are easy to compute with explicit formulas [4]. The dimensions of the room are 5.56 m x 3.97 m x 2.81 m. There are 25 source-receiver-pairs (5 sources and 5 receivers). Only one typical pair is shown here, where the source position is (2.09, 2.12, 2.12) m and the receiver position (2.09, 3.08, 0.96) m. A low frequency modal analysis is performed three times where the reflection coefficients of all surfaces are set to 0.8, 0.9, and 0.999 respectively.

Figure 1 compares FDTD results with the geometric modeling results. The FDTD scheme used in this case is the standard rectilinear scheme. The geometric results are produced with image sources which are trivial to calculate in the case of this model. It can be seen that after the calibration, the levels of the resulting impulse responses are very close to each other. Most of the differences can be attributed to the differences in the boundary model.

4. CONCLUSIONS

It is suitable to model low frequencies with a FDTD algorithm, because all wave phenomena are properly modelled. At higher frequencies, the grid size becomes too large for practical applications. In addition, many FDTD schemes suffer from dispersion error which becomes more prominent at long distances or, equivalently, with dense grids required for high frequency modeling. Thus, it is advisable to use faster methods that do not cause dispersion at high frequencies. Geometric methods fulfill these requirements. On the other hand, they do not model all the wavephenomena that FDTD algorithms model. It is reasonable to conclude that hybrid modeling can produce more accurate results in a given time with limited computing resources.

To combine the results produced with different algorithms, the source signals must be calibrated to the same level. This is achieved by recording the signal at the receiver position right next to the source and using the DC level of that signal to adjust it accordingly. This simulation is required only once per FDTD scheme, not once per room geometry. Thus, it is useful to have the simulation results available as numbers as in Table 1. Then, it is sufficient to plug the appropriate number into Eq. 8, and scale the FDTD results with the calibration factor.

Finally, it is also worth noting that the calibration parameter is necessary when comparing the results of different FDTD schemes directly.

5. ACKNOWLEDGEMENT

The research leading to these results has received funding from the Academy of Finland, project no. [138780].

6. REFERENCES

[1] K. Kowalczyk, and M. van Walstijn, "Room Acoustics Simulation Using 3-D Compact Explicit FDTD Schemes," *IEEE Transactions on Audio, Speech, and Language Processing*, 19(1): 34-46, 2011.

[2] S. Siltanen, T. Lokki, S. Kiminki, and L. Savioja, "The Room Acoustic Rendering Equation," *Journal of the Acoustical Society of America*, 122(3): 1625-1635, 2007.

[3] Z. Chen and R. C. Maher, "Analytical Expression for Impulse Response Between Two Nodes in 2-D Rectangular Digital Waveguide Mesh," *IEEE Signal Processing Letters*, 15:221-224, 2008.

[4] H. Kuttruff, "Room Acoustics", Spon Press, London, England, 4th edition, 2000.

[5] B.-I. Dalenbäck, "Room Acoustics Prediction Based on a Unified Treatment of Diffuse and Specular Reflection," *Journal of the Acoustical Society of America*, 100(2): 899-909, 1996.

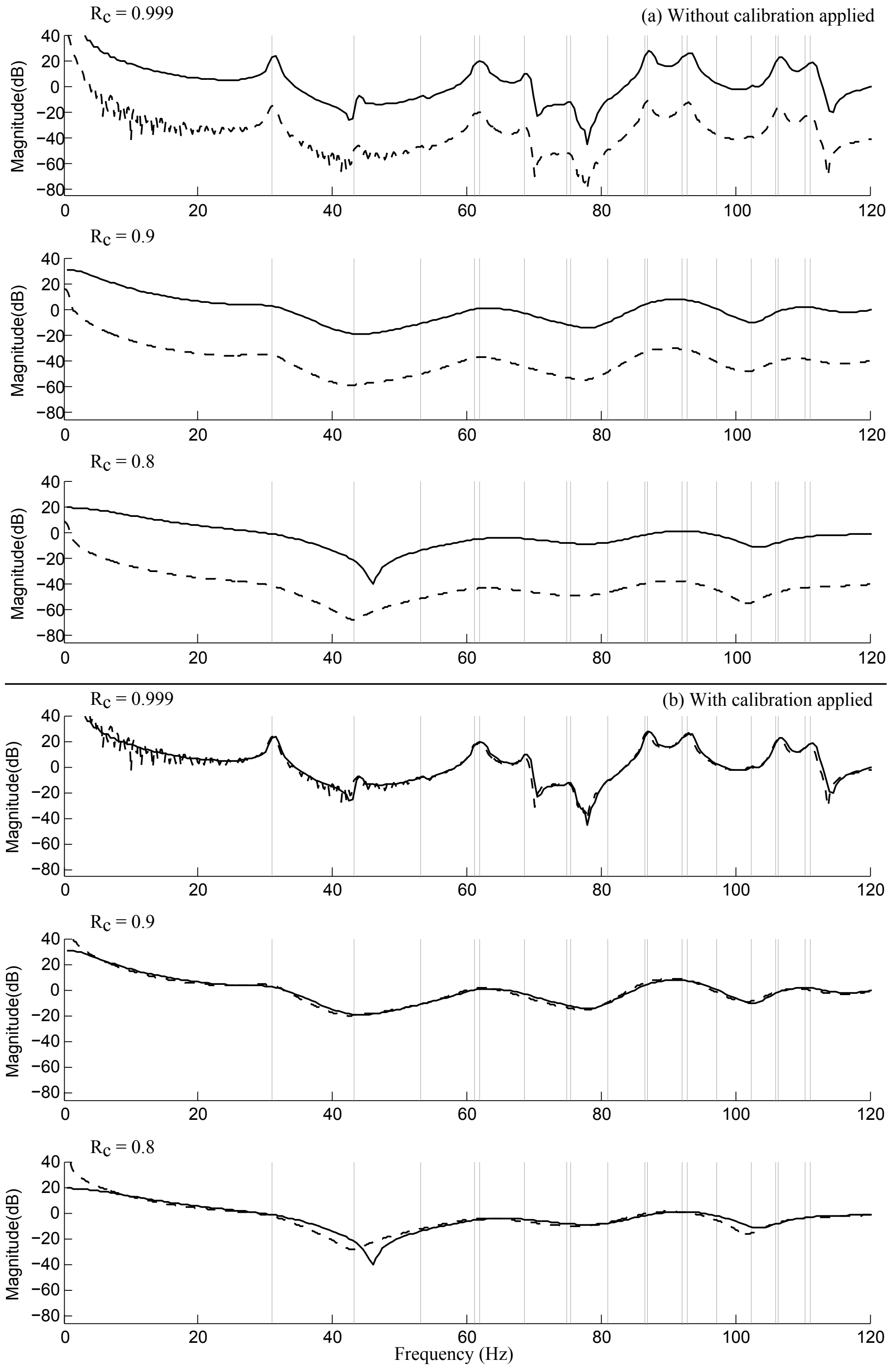

Fig. 1. Comparison of modal responses as produced with a FDTD algorithm (dotted) and geometric acoustics modeling (solid). The comparison is made for three different reflection coefficients, R_c (0.8, 0.9, or 0.999) without and with the calibration applied in (a) and (b) respectively. Vertical lines indicate the expected analytical modal resonances of the cuboid room dimensions.

[6] T. Lewers, “A Combined Beam Tracing and Radiant Exchange Computer Model of Room Acoustics,” *Applied Acoustics*, 38(2-4): 161-178, 1993.

[7] M. Vorländer, “Simulation of the Transient and Steady-State Sound Propagation in Rooms using a New Combined Ray-Tracing/Image-Source Algorithm,” *Journal of the Acoustical Society of America*, 86(1): 172-178, 1989.

[8] U. P. Svensson and U. R. Kristiansen, “Computational Modelling and Simulation of Acoustic Spaces,” *Proc. of the 22nd AES Internation Conference on Virtual, Synthetic and Entertainment Audio*, Helsinki, Finland, June 15-17, 2002, pp. 1-20.

[9] V. Välimäki, J. D. Parker, L. Savioja, J. O. Smith III, J. S. Abel, ”Fifty Years of Artificial Reverberation,” *IEEE Transactions on Audio, Speech, and Language Processing*, 20(5): 1421-1448, 2012.

[10] D.T. Murphy, M. Beeson, S. Shelley, A. Southern, and A. Moore, “Hybrid Room Impulse Response Synthesis in Digital Waveguide Mesh Based Room Acoustics Simulation”, *Proc. of the 11th Int. Conf. on Digital Audio Effects (DAFx-08)*, Espoo, Finland, Sept. 1-4, 2008, pp. 129-136.

[11] M. Aretz, R. Nöthen, M. Vorländer, and D. Schröder, “Combined Broadband Impulse Responses Using FEM and Hybrid Ray-Based Methods”, *Proc. of the EAA Auralization Symposium 2009*, Espoo, Finland, 15th-17th Jun., 2009.

[12] A. Southern, S. Siltanen, and L. Savioja, “Spatial Room Impulse Responses with a Hybrid Modelling Method,” *Proc. of the 130th AES Convention* London, UK, May 13-16, 2011, Convention Paper 8385.